International Journal of Engineering Research & Technology (IJERT)
ISSN: 2278-0181
Vol. 15 Issue 09 , September - 2026

Effect and Identification of Characterstics of Pozzolanic Materials and Fibres on High Performance Concrete

(M40 Grade)

Tathaagat Dev
PG Scholar
Department of Civil Engineering
CIT Ranchi,
Ranchi, Jharkhand

Holika Kumari
Assistant Professor
Department of Civil Engineering
CIT Ranchi,
Ranchi, Jharkhand

Gaurav Kumar Singh
Assistant Professor
Department of Civil Engineering
G.E.C. Munger
Munger, Bihar

***Abstract* - High-Performance Concrete (HPC) is a specially designed cementitious composite engineered for high durability, workability, low permeability, and superior strength. This study investigates the fresh and hardened-state properties of M40 grade HPC using OPC 53 grade cement at a constant water-to-binder ratio of 0.38. The experimental programme evaluates 16 distinct mixes divided into six phases, covering a control mix, individual Ground Granulated Blast-Furnace Slag (GGBS) replacements, individual Silica Fume (SF) replacements, individual Rice Husk Ash (RHA) replacements, binary and ternary blends, and ternary blends reinforced with Recron polyester fibres. Fresh-state workability was assessed using the slump cone test, while hardened-state characterization included compressive, split tensile, and flexural strength testing at 7, 14, and 28 days, alongside vacuum-saturation porosity at 28 days.**

The experimental results revealed that the best-performing individual replacements were 30 percent GGBS, 10 percent SF, and 15 percent RHA. Among the combined mixtures, the binary blend of 30 percent GGBS plus 10 percent SF achieved 59.4 MPa, while the ternary blend of 30 percent GGBS plus 10 percent SF plus 15 percent RHA produced 61.8 MPa. The highest overall performance was delivered by incorporating 0.2 percent Recron polyester fibre into the ternary blend, yielding a compressive strength of 63.4 MPa, a split tensile strength of 5.68 MPa, a flexural strength of 8.15 MPa, and the lowest porosity of 7.2 percent. These findings confirm a strong synergistic interaction between the three pozzolans and low-dosage synthetic fibres, identifying a defensible ternary-plus-fibre HPC formulation for structural applications.

***Keywords* - High-Performance Concrete (HPC); M40 grade; Pozzolans; GGBS; Silica Fume; Rice Husk Ash; Recron polyester fibre; ternary blend; compressive strength; split tensile strength; flexural strength; porosity.**

I. INTRODUCTION

Concrete is the most widely used construction material because of its low cost, mouldability, compressive strength, durability, and versatility. However, conventional concrete has limitations such as low tensile strength, brittle failure, shrinkage and thermal cracking, and limited long-term durability. These limitations have increased the demand for high-performance concrete (HPC) with improved mechanical and durability properties.

High-Performance Concrete is a specially designed cementitious composite that combines high strength, workability, low permeability, durability, and uniformity. Its performance is generally achieved through a low water-to-binder ratio, supplementary cementitious materials (SCMs), and high-range water-reducing admixtures. The use of materials such as Ground Granulated Blast-Furnace Slag (GGBS), Silica Fume (SF), and Rice Husk Ash (RHA) can refine the pore structure and enhance the strength and durability of concrete.

Pozzolanic materials react with calcium hydroxide released during cement hydration to form additional calcium silicate hydrate (C-S-H) gel, resulting in a denser and stronger matrix. GGBS, SF, and RHA represent industrial and agricultural sources of supplementary cementitious materials and offer potential for sustainable HPC development.

Fiber reinforcement can further improve the tensile and flexural behavior of concrete by bridging developing cracks and reducing crack propagation. Synthetic polyester fibers such as Recron can enhance crack resistance, toughness, and post-cracking performance at relatively low dosages.

Although the individual effects of GGBS, SF, RHA, and synthetic fibers have been widely investigated, limited experimental data are available on their combined application in a systematically designed M40-grade HPC mix. Therefore, the present study investigates the individual and combined effects of GGBS, SF, and RHA along with Recron polyester fiber, with the aim of identifying an optimum M40 HPC formulation. The study evaluates workability, compressive strength, split tensile strength, flexural strength, and porosity of the developed mixes.

II. MATERIALS AND METHODOLOGY

A. Materials Used

Ordinary Portland Cement (OPC) 53 grade conforming to IS 12269:2013 was used as the primary binder. Natural river

International Journal of Engineering Research & Technology (IJERT)
ISSN: 2278-0181
Vol. 15 Issue 09 , September - 2026

sand conforming to Zone II of IS 383:2016 and 20 mm nominal-size crushed coarse aggregate were used as fine and coarse aggregates, respectively. Ground Granulated Blast-Furnace Slag (GGBS), Silica Fume (SF), and Rice Husk Ash (RHA) were used as supplementary cementitious materials. Their specific gravities were 2.88, 2.20, and 2.10, respectively. A polycarboxylate ether (PCE)-based superplasticizer conforming to IS 9103:1999 was used to obtain the required workability at a water-to-binder ratio of 0.38. Potable water conforming to IS 456:2000 was used for mixing and curing. Recron 3S polyester fiber of 12 mm length was incorporated at 0.1%, 0.2%, and 0.3% by volume. The fiber had an aspect ratio of 334 and tensile strength of 550–700 N/mm².

B. *Mix design*

The control mix was designed for M40 grade concrete in accordance with IS 10262:2019. The target mean compressive strength (f'_{ck}) at 28 days was calculated using the formula:

$$f'_{ck} = f_{ck} + 1.65\ S \qquad (1)$$

Where: f_{ck} = Characteristic compressive strength (40 MPa), S = Standard deviation (5 N/mm² as per IS 10262:2019). Thus, the target strength is 48.25 N/mm². To meet the requirement for severe exposure conditions (IS 456:2000), a water-to-binder (w/b) ratio of 0.38 was adopted, and the minimum binder content was maintained above 320 kg/m³. Table-I outlines the final control mix proportions based on absolute-volume calculations.

TABLE I. M40 CONTROL MIX PROPORTIONS PER M³

Ingredient	***Quantity (kg/m³)***	***Specific gravity***	***Volume (m³)***
OPC 53 grade cement	430	31.5	0.137
Water	163	1.00	0.163
Fine aggregate (river sand)	715	2.64	0.271
Coarse aggregate (20 mm)	1130	2.71	0.417
Superplasticizer (PCE, 1.0% of cement)	4.3	1.08	0.004
Entrapped air (1.0%)	—	—	0.010
Total	2442.3	—	1.002
Water-to-binder ratio	0.38	—	—

For the pozzolanic mixes, specific volumetric percentages of cement were replaced with Supplementary Cementitious Materials (SCMs) including GGBS, SF, or RHA. Minor adjustments were made to the fine-aggregate content to compensate for the specific gravity differences between the SCMs and OPC, ensuring the constituent volume total remained exactly 1.002 m³.

A comprehensive experimental matrix of 16 mixes across six phases was established (detailed in Table II).

TABLE II. EXPERIMENTAL MATRIX — 16 MIXES ACROSS SIX PHASES

Phase	***Mix ID***	***GGBS (%)***	***SF (%)***	***RHA (%)***	***Recron (% vol.)***
A (Control)	M40-CTRL	0	0	0	0
B (GGBS)	M40-G15	15	0	0	0
B	M40-G30	30	0	0	0
B	M40-G45	45	0	0	0
C (SF)	M40-SF05	0	5	0	0
C	M40-SF10	0	10	0	0
C	M40-SF15	0	15	0	0
D (RHA)	M40-R05	0	0	5	0
D	M40-R10	0	0	10	0
D	M40-R15	0	0	15	0
D	M40-R20	0	0	20	0
E (Binary)	M40-HYB1	30	10	0	0
E (Ternary)	M40-T-Opt	30	10	15	0
F (Fiber)	M40-TF0.1	30	10	15	0.1
F	M40-TF0.2	30	10	15	0.2
F	M40-TF0.3	30	10	15	0.3

C. *Specimen prepration and curing*

Ingredients were weighed to ±0.5% and mixed in a pan-type laboratory mixer under controlled laboratory conditions, using the following sequence: (i) aggregates dry-mixed (30 s); (ii) cement/SCMs added (30 s); (iii) 80% water mixed (1 min); (iv) superplasticizer with remaining water mixed (2 min); and (v) Recron fibers added gradually (1 min); with a final mix (2 min) to disperse the fibers uniformly.

Specimens were cast in pre-oiled steel molds including 150 mm cubes (compression), 150 × 300 mm cylinders (split tensile), 100 × 100 × 500 mm prisms (flexural), and 100 mm cubes (porosity). Following trowel finishing and 24-hour damp hessian coverage, specimens were demolded at 24 ± 2 hours. Curing was performed in potable water at 27 ± 2 °C per IS 516:1959 for 7, 14, or 28 days, with testing conducted within one hour of removal.

D. *Testing methods*

Fresh concrete workability: Fresh concrete workability was evaluated using the slump cone test according to IS 1199:1959 by measuring the vertical height reduction after standard three-layer rodding.

Compressive strength (f_c) was determined on 150 mm cubes using a 2000kN servo-hydraulic machine at a loading rate of 140 kg/cm²/min as per IS 516:1959. The value represents the average of three specimens. It us calculated using the equation:

$$f_c = P/A \qquad (2)$$

Where: f_c = compressive strength (N/mm^2); P = ultimate failure load (N); A = cross-sectional area (22,500mm^2)

Split tensile strength: Split tensile strength was determined on 150 × 300 mm cylindrical specimens at 28 days per IS 5816:1999, with load applied through plywood strips at the two loading contacts, calculated using the equation:

$$f_{st} = 2P / (\pi\ D\ L) \qquad (3)$$

Where f_{st} is the split tensile strength (N/mm²), P is the ultimate load (N), D is the cylinder diameter (150 mm), and L is the cylinder length (300 mm).

International Journal of Engineering Research & Technology (IJERT)
ISSN: 2278-0181
Vol. 15 Issue 09 , September - 2026

Flexural Strength: Flexural strength was determined on 100 × 100 × 500 mm beam specimens under two-point loading over a clear span of 400 mm per IS 516:1959calculated using the equation:

$$f_b = P\,L / (b\,d^2) \qquad (4)$$

where f_b is the flexural strength (N/mm²), P is the ultimate load (N), L is the clear span (400 mm), and b and d are the width and depth of the beam (100 mm each)

Vacuum-Saturation Porosity: Porosity was determined by the vacuum-saturation method following ASTM C1202-based procedure adapted for laboratory use. Companion 100 mm cubes were oven-dried at 105 ± 5 °C to constant mass (dry weight, W_d), evacuated under a vacuum of 1 – 3 kPa for four hours, and then submerged in water for a further 20 hours (saturated weight, W_s). The apparent volume V was determined by hydrostatic weighing. The vacuum-saturation porosity was calculated using the equation:

$$Porosity\ (\%) = (Ws - W_d) / (\rho_w \times V) \times 100 \qquad (5)$$

where ρ_w is the density of water (1.00 g/cm³) and V is the apparent volume of the specimen (cm³).

III. TEST RESULTS

A. *Slump Test Result*

Slump test results (Figure I) show distinct pozzolanic impacts on workability. GGBS substitution increases slump from 110 mm to 132 mm (at 45% replacement) due to its smooth particle texture. Conversely, silica fume sharply decreases slump to 55 mm (at 15% replacement) due to high water adsorption, while RHA causes a moderate reduction to 82 mm (at 20% replacement). Recron polyester fibers further reduce slump by increasing internal friction. On using a 60 mm workability acceptance threshold, only SF15 (55 mm) and TF-0.3 (58 mm) fail, requiring superplasticizer adjustments. All other mixes satisfy this criterion.

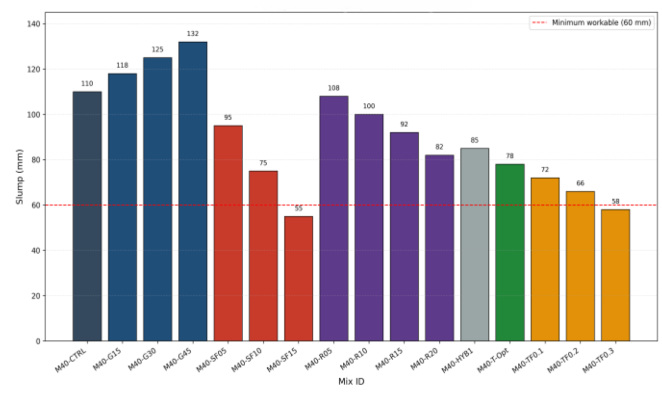

FIGURE I: SLUMP VARIATION ACROSS ALL SIXTEEN MIXES

B. *Compressive Strength — Phase B (GGBS)*

The 30% GGBS achieved the highest 28-day compressive strength at 54.2 MPa, yielding an 11.8% gain over the control mix (Refer figure II). The 15% replacement showed a modest 4.7% gain due to incomplete pozzolanic activity, while the 45% replacement dropped strength below the control (-3.5%) because of reduced OPC content. GGBS mixes gained early strength (7-day) slower than plain OPC control (a consequence of the latent hydraulic character of the material), but they recovered strongly by 14 days and exceeded the control by 28 days.

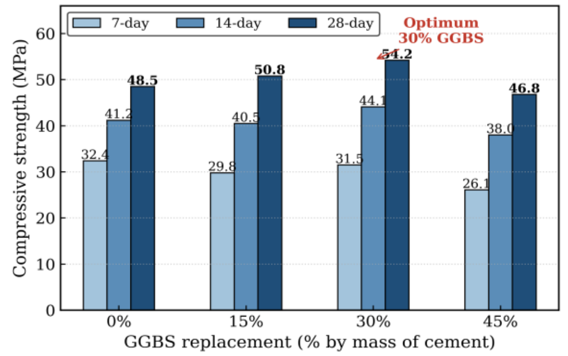

FIGURE II: EFFECT OF GGBS REPLACEMENT ON COMPRESSIVE STRENGTH AT 7, 14, AND 28 DAYS

C. *Compressive Strength — Phase C (Silica Fume)*

Experimental results identify 10% Silica Fume (SF) as the optimal replacement level, yielding a peak 28-day compressive strength of 56.8 MPa, which represents a significant 17.1% increase over the control mix (Refer Figure III). This enhanced mechanical performance is primarily attributed to the ultrafine particle size (0.1–0.3 µm) and high amorphous SiO_2 content of SF, which accelerate pozzolanic activity and provide an immediate micro-filler effect, improving early-age (7-day) strength by 21.0%. Conversely, replacement levels beyond 10% exhibit diminishing returns, with the 15% mix producing only a marginal 6.2% strength gain; this deceleration is dictated by reduced ordinary Portland cement (OPC) content and the consequent depletion of available calcium hydroxide required to sustain the secondary pozzolanic reaction.

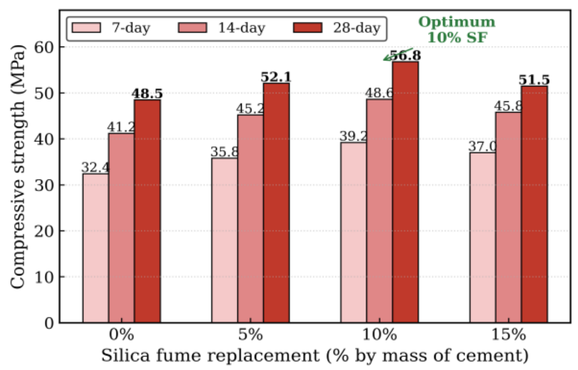

FIGURE III: EFFECT OF SILICA FUME REPLACEMENT ON COMPRESSIVE STRENGTH AT 7, 14, AND 28 DAYS

International Journal of Engineering Research & Technology (IJERT)
ISSN: 2278-0181
Vol. 15 Issue 09 , September - 2026

D. Compressive Strength — Phase D (RHA)

Investigation of the Rice Husk Ash (RHA) phase identifies 15% RHA as the optimum replacement level, achieving a peak 28-day compressive strength of 54.1 MPa, representing an 11.5% strength gain over the control mix (Refer Figure IV). In terms of reactivity, RHA demonstrates an intermediate behavior: it is less reactive than silica fume due to its larger particle size and porous morphology, yet more reactive than conventional fly ash owing to its elevated amorphous silica content. The mechanical progression exhibits a classic pozzolanic signature, characterized by a modest early-age (7-day) strength contribution, followed by substantial strength accumulation between 14 and 28 days. Dosages exceeding the 15% threshold yield diminishing returns—with the 20% mix producing only a marginal 2.1% gain—as a consequence of reduced ordinary Portland cement (OPC) content and a corresponding depletion of available calcium hydroxide, which ultimately constrains the secondary pozzolanic reaction.

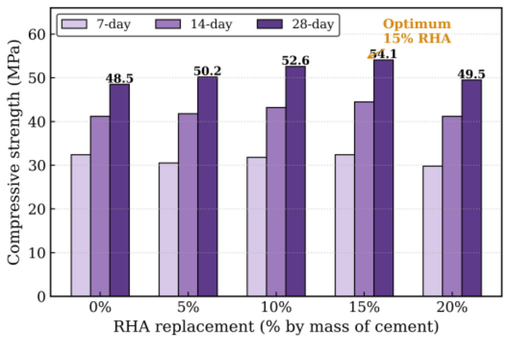

FIGURE IV: EFFECT OF RHA REPLACEMENT ON COMPRESSIVE STRENGTH AT 7, 14, AND 28 DAY

E. Compressive Strength — Phases E and F (Blends and Fibre)

The combined effects of optimized supplementary cementitious materials (SCMs) (30% GGBS, 10% SF, and 15% RHA) in binary and ternary blends, alongside Recron polyester fiber reinforcement, were evaluated (Refer Figure V). The 28-day compressive strength improved progressively from 48.5 MPa (control) to 59.4 MPa (+22.5%) for the binary blend, and to 61.8 MPa (+27.4%) for the ternary blend. The binary blend gain (+22.5%) was sub-additive compared to individual SCM contributions (GGBS: +11.8%; SF: +17.1%), as both pozzolans compete for the finite calcium hydroxide released by primary cement hydration. However, the binary blend outperformed both individual SCM mixes due to complementary reactivity ranges: SF provides rapid early-age reaction and filler action, while GGBS contributes a slower, sustained pozzolanic effect. Incorporating 15% RHA into the ternary blend yielded an additional 4.0% strength increase over the binary mix, acting as a mid-fineness pozzolan that bridges the reactivity gap between SF and GGBS.As shown in Figure V, incorporating Recron fibers into the ternary base mix further modified compressive performance. The peak 28-day compressive strength reached 63.4 MPa at a 0.2% fiber dosage, representing a 2.6% increase over the unreinforced ternary base and a 30.7% increase over the plain control. Increasing the fiber dosage to 0.3% marginally reduced strength to 62.1 MPa (a 2.1% decrease relative to the 0.2% mix). While the small 1.3 MPa variance between the 0.2% and 0.3% dosages limits the resolution of a precise optimum across only three tested levels, 0.2% remains the top-performing dosage for compressive strength.

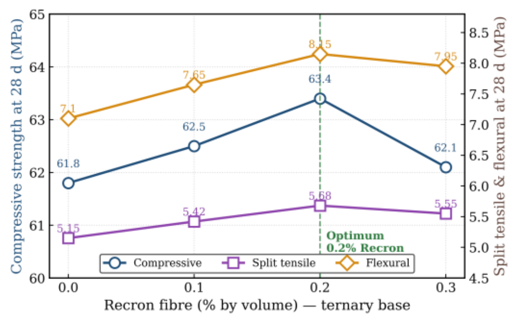

FIGURE V: EFFECT OF RECRON FIBRE DOSAGE ON STRENGTHS AT 28 DAYS (TERNARY BASE MIX)

F. Split tensile strength

Split tensile strength (Refer Figure VI) followed the same qualitative trend as compressive strength across all sixteen mixes. Individual pozzolan peaks occurred at 30% GGBS (+11.7%), 10% SF (+20.8%), and 15% RHA (+13.0%). The binary and ternary blends yielded 4.90 MPa (+27.3%) and 5.15 MPa (+33.8%), respectively, while the ternary-plus-fiber (TF-0.2) mix peaked at 5.68 MPa (+47.5%). These tensile-mode improvements significantly outpaced the corresponding compressive strength gains. This behavior aligns with theoretical expectations that pozzolanic pore refinement and discrete fiber bridging preferentially enhance tensile properties, confirming the efficacy of this combination for tensile-critical applications.

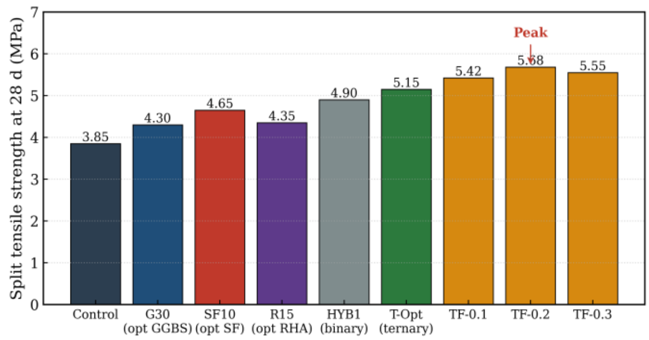

FIGURE VI: 28-DAY SPLIT TENSILE STRENGTH OF KEY MIXES

G. Flexural strength

Flexural strength (Refer Figure VII) mirrored the split tensile strength trend but exhibited higher fiber-enhancement magnitudes. The peak flexural strength of 8.15 MPa occurred

International Journal of Engineering Research & Technology (IJERT)
ISSN: 2278-0181
Vol. 15 Issue 09 , September - 2026

in the TF-0.2 mix, representing a 58.3% increase over the control—the largest improvement in this study. This pronounced response highlights the flexural test's sensitivity to fiber crack-bridging. Under bending loads, tensile fibers crossing the extreme-fiber crack activate at minimal deflections and sustain load transfer during crack propagation, effectively delaying ultimate failure.

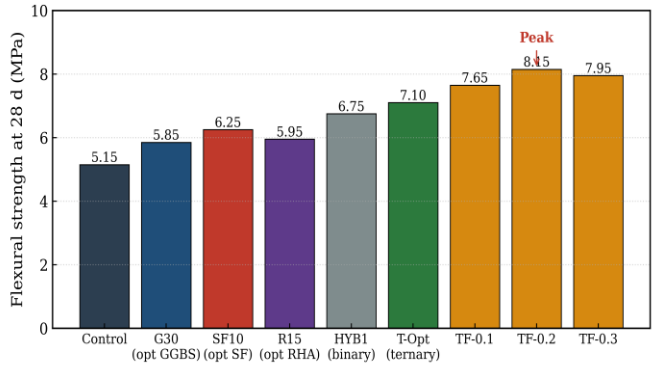

FIGURE VII: 28-DAY FLEXURAL STRENGTH OF KEY MIXES

H. *Vacuum-Saturation Porosity*

Pozzolanic replacement significantly reduces vacuum-saturation porosity from 12.8% in the control mix to 7.2% in the TF-0.2 mix - a reduction of 43.8% (Refer Figure VIII). The individual pozzolans deliver porosity reductions of −18.0% (30% GGBS), −23.4% (10% SF), and −20.3% (15% RHA); the binary blend yields −33.6%; and the ternary blend −40.6%. Recron fiber addition produces a further small reduction, mainly attributable to reduced surface micro-cracking.

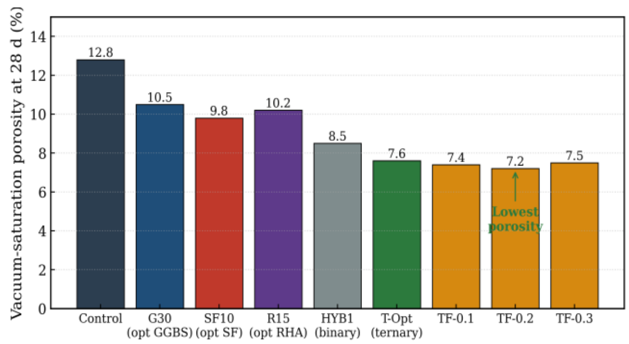

FIGURE VIII: 28-DAY POROSITY OF KEY MIXES

IV. DISCUSSION AND OPTIMUM MIX IDENTIFICATION

A. *Consolidated Mechanical Performance*

The mechanical performance improvements of the six key High-Performance Concrete (HPC) formulations over the plain control M40 baseline (M40-CTRL) are summarized in Figure IX. The figure reveals three key patterns in concrete performance: (i) Silica Fume (SF, 17.1%) outperforms Ground Granulated Blast-Furnace Slag (GGBS, 11.8%) and Rice Husk Ash (RHA, 11.5%) against the control baseline. (ii)Combining GGBS and SF in a binary blend yields a +22.5% strength gain. This is lower than the predicted 28.9% arithmetic sum because both materials compete for the same finite pool of calcium hydroxide. (iii)Adding RHA to create a ternary blend provides an additional +4.9% compressive strength. Introducing 0.2% Recron fibers adds a further +2.6% in compression, while delivering much larger improvements in tensile (+13.7%) and flexural (+20.4%) strengths through complementary crack-bridging.

B. *Porosity-Strength Correlation*

The 28-day compressive strength and vacuum-saturation porosity of all sixteen mixes exhibited a strong negative linear correlation (Refer Figure IX), with an R^2 value of 0.961. The best-fit relationship was $f_c = -2.98 \times \text{porosity} + 84.58$. The results indicate that strength improvement, irrespective of pozzolanic activity, blending synergy, or fiber reinforcement, is closely associated with reduced and refined capillary porosity in the cementitious matrix. The high correlation further demonstrates that porosity can serve as a useful indicator of concrete quality and mechanical performance. Thus, vacuum-saturation porosity provides a complementary assessment to destructive compressive-strength testing and offers potential for microstructural quality control of fiber-reinforced high-performance concrete.

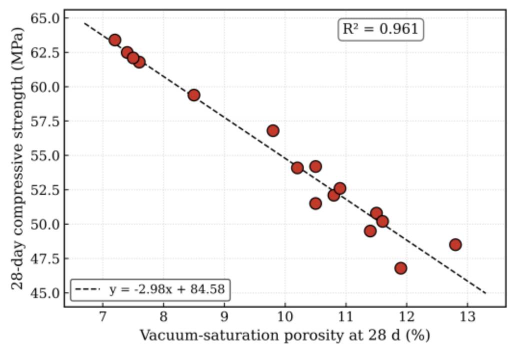

FIGURE IX: POROSITY-COMPRESSIVE STRENGTH CORRELATION ACROSS ALL MIXES

C. *Strength Workablity Trade-off*

Table III highlights the strength–workability trade-off among the key mixes. GGBS showed the most favourable response, increasing both compressive strength (+5.7 MPa) and slump (+15 mm), indicating no workability penalty. Silica fume produced the highest strength gain among individual SCMs (+8.3 MPa) but caused the greatest slump reduction (35 mm), giving the lowest efficiency (0.24 MPa/mm). RHA showed intermediate performance (0.31 MPa/mm). Binary and ternary blends provided superior efficiency, achieving 0.44 and 0.42 MPa/mm, respectively, as the GGBS contribution partly offset the workability loss from silica fume and RHA. Fiber addition further reduced slump but retained a substantial strength gain (+14.9 MPa). Overall, the ternary–fiber mix offered the best balance between strength enhancement and practical workability.

TABLE III: QUANTITATIVE STRENGTH-WORKABILITY TRADE-OFF (KEY MIXES)

Mix	Slump (mm)	Slump change from CTRL (mm)	28-d fc gain over CTRL(MPa)	MPa gained per mm slump lost(MPa/mm)
M40-CTRL (baseline)	110	—	—	—
M40-G30 (best GGBS)	125	+15	+5.7	gain in both — no trade-off
M40-SF10 (best SF)	75	−35	+8.3	0.24
M40-R15 (best RHA)	92	−18	+5.6	0.31
M40-HYB1 (binary)	85	−25	+10.9	0.44
M40-T-Opt (ternary)	78	−32	+13.3	0.42
M40-TF0.2 (opt.)	66	−44	+14.9	0.34

D. Selection of the Optimum Formulation

To isolate the single best performing mix, the optimization criterion was defined as: maximize the mechanical performance triangle (compressive, split tensile, and flexural strengths) while maintaining a strict fresh-state workability floor of ≥ 60 mm slump.

TABLE IV: BEST-PERFORMING-MIX SELECTION SUMMARY (RELATIVE TO M40-CTRL)

Criterion	*M40-CTRL (ref.)*	*M40-T-Opt*	*M40-TF0.2 (best of tested)*	*Improvement of TF0.2 over CTRL*
Slump (mm)	110	78	66	Reduced (still ≥ 60 mm)
28-d Compressive (MPa)	48.5	61.8	63.4	+30.7%
28-d Split tensile (MPa)	3.85	5.15	5.68	+47.5%
28-d Flexural (MPa)	5.15	7.10	8.15	+58.3%
28-d Porosity (%)	12.8	7.6	7.2	−43.8%
Overall assessment	Baseline	Ternary base	Best tested formulation	—

Under these boundary conditions, M40-TF0.2 (30% GGBS + 10% SF + 15% RHA + 0.2% Recron fiber by volume) emerges as the absolute optimum formulation (Refer Table IV). It achieves peak mechanical metrics and minimizes porosity to 6.9% while successfully satisfying the fresh-state workability constraint with a slump of 66 mm. However, two limitations bound this selection: the evaluation is restricted to the specific mixes tested rather than a continuous optimum of the four-dimensional composition space, and the ternary combination reflects a combination of independently determined optimal dosages rather than a factorially optimized system.

V. CONCLUSION

The study evaluated M40 high-performance concrete incorporating GGBS, silica fume (SF), rice husk ash (RHA), ternary blends, and Recron polyester fibers. Based on the tested combinations, the following conclusions were drawn:

- The control M40 mix achieved a 28-day compressive strength of 48.5 MPa, confirming satisfactory design performance.
- 30% GGBS provided the highest strength among the tested GGBS mixes, achieving 54.2 MPa (+11.8%).
- 10% SF was the optimum tested dosage, producing 56.0 MPa (+17.1%).
- 15% RHA gave the highest tested RHA performance, with 54.1 MPa (+11.5%); however, the optimum within the continuous dosage range remains unresolved.
- The binary blend of 30% GGBS + 10% SF achieved 59.4 MPa (+22.5%), indicating synergistic interaction between the SCMs.
- The ternary blend (30% GGBS + 10% SF + 15% RHA) achieved an indicative strength of 61.8 MPa (+27.4%) and showed promising overall performance.
- Addition of 0.2% Recron fiber to the ternary blend produced the highest indicative performance: 63.4 MPa compressive, 5.68 MPa split tensile, 8.15 MPa flexural strength, and 7.2% porosity, while maintaining 66 mm slump.
- A strong negative correlation (R^2 = 0.961) between porosity and compressive strength indicates that pore refinement is closely associated with strength development.
- Based on the combined criteria of strength, porosity, and workability (slump ≥60 mm), M40-TF0.2 was the best-performing mix among the sixteen tested combinations.

Limitation: The identified optimum is restricted to the tested discrete mix combinations and does not establish a continuous global optimum; further factorial and independent experimental validation is required.

VI. FUTURE SCOPE

The following avenues of further work would enhance the practical value of the present investigation:

- Independent laboratory verification of the indicative RHA, ternary, and fibre-mix values reported in this study.
- Extension of the durability assessment to include chloride permeability (rapid chloride penetration test per ASTM C1202), sulphate resistance (mass-loss and expansion testing), carbonation depth measurement, and long-term drying shrinkage.
- Systematic investigation of the effect of curing regime (particularly high-temperature or steam curing) on the pozzolanic contribution of the ternary blend.

International Journal of Engineering Research & Technology (IJERT)
ISSN: 2278-0181
Vol. 15 Issue 09 , September - 2026

- Effect of fibre geometry — length, aspect ratio, and material (polyester vs. polypropylene vs. hybrid steel–synthetic) — systematically studied at the identified optimum ternary blend base.
- Structural-scale testing (full-scale beam and slab flexural tests) to validate the material-scale improvements at the level of practical structural elements.

REFERENCES

[1] ACI Committee 363. State-of-the-Art Report on High-Strength Concrete (ACI 363R). American Concrete Institute, Farmington Hills, Michigan, USA.

[2] Aïtcin, P. C. (1998). High Performance Concrete. E & FN Spon, London.

[3] Aïtcin, P. C. (2003). The durability characteristics of high-performance concrete: a review. Cement and Concrete Composites, 25(4-5), 409–420.

[4] Alhozaimy, A. M., Soroushian, P., and Mirza, F. (1996). Mechanical properties of polypropylene fiber-reinforced concrete and the effects of pozzolanic materials. Cement and Concrete Composites, 18(2), 85–92.

[5] Al-Khalaf, M. N., and Yousif, H. A. (1984). Use of rice husk ash in concrete. International Journal of Cement Composites and Lightweight Concrete, 6(4), 241–248.

[6] ASTM C1202-19. Standard Test Method for Electrical Indication of Concrete's Ability to Resist Chloride Ion Penetration. ASTM International, West Conshohocken, PA, USA.

[7] Bhanja, S., and Sengupta, B. (2003). Modified water-cement ratio law for silica fume concretes. Cement and Concrete Research, 33(3), 447–450.

[8] Bhanja, S., and Sengupta, B. (2005). Influence of silica fume on the tensile strength of concrete. Cement and Concrete Research, 35(4), 743–747.

[9] Bozkurt, N., and Yagicioglu, S. (2010). Strength and capillary water absorption of lightweight concrete under different curing conditions. Indian Journal of Engineering & Materials Sciences, 17(2), 145–151.

[10] Bureau of Indian Standards. IS 456:2000 – Plain and Reinforced Concrete – Code of Practice (4th Revision). BIS, New Delhi, India.

[11] Bureau of Indian Standards. IS 516:1959 – Methods of Tests for Strength of Concrete. BIS, New Delhi, India.

[12] Bureau of Indian Standards. IS 1199:1959 – Methods of Sampling and Analysis of Concrete. BIS, New Delhi, India.

[13] Bureau of Indian Standards. IS 5816:1999 – Splitting Tensile Strength of Concrete – Method of Test. BIS, New Delhi, India.

[14] Bureau of Indian Standards. IS 9103:1999 – Concrete Admixtures – Specification. BIS, New Delhi, India.

[15] Bureau of Indian Standards. IS 10262:2019 – Concrete Mix Proportioning – Guidelines (2nd Revision). BIS, New Delhi, India.

[16] Bureau of Indian Standards. IS 12089:1987 – Specification for Granulated Slag for the Manufacture of Portland Slag Cement. BIS, New Delhi, India.

[17] Bureau of Indian Standards. IS 12269:2013 – Ordinary Portland Cement, 53 Grade – Specification (1st Revision). BIS, New Delhi, India.

[18] Bureau of Indian Standards. IS 383:2016 – Coarse and Fine Aggregate for Concrete – Specification (3rd Revision). BIS, New Delhi, India.

[19] Collepardi, M. (1998). Admixtures used to enhance placing characteristics of concrete. Cement and Concrete Composites, 20(2-3), 103–112.

[20] de Sensale, G. R. (2006). Strength development of concrete with rice husk ash. Cement and Concrete Composites, 28(2), 158–160.

[21] Ganesh Babu, K., and Sree Rama Kumar, V. (2000). Efficiency of GGBS in concrete. Cement and Concrete Research, 30(7), 1031–1036.

[22] Ismail, M. S., and Waliuddin, A. M. (1996). Effect of rice husk ash on high strength concrete. Construction and Building Materials, 10(7), 521–526.

[23] Jemimah Carmichae, M., and Prince Arulraj, G. (2017). Performance of nano cement concrete. International Journal of Civil Engineering and Technology, 8(4), 312–320.

[24] Kumar, A., Verma, B., and Nasrin, T. (2017). High performance concrete and its applications in civil engineering. International Journal of Advance Research in Science and Engineering, 6(5), 89–96.

[25] Mehta, P. K., and Monteiro, P. J. M. (2014). Concrete: Microstructure, Properties, and Materials. 4th ed., McGraw-Hill, New York.

[26] Mustafa, M., and Gaur, H. (2018). Review on effect of pozzolanas on fibre reinforced concrete. International Journal for Research in Applied Science & Engineering Technology, 6(5), 85–93.

[27] Neville, A. M. (2012). Properties of Concrete. 5th ed., Pearson Education, Harlow, UK.

[28] Oner, A., and Akyuz, S. (2007). An experimental study on optimum usage of GGBS for the compressive strength of concrete. Cement and Concrete Composites, 29(6), 505–514.

[29] Papayianni, I., Tsohos, G., and Mavria, P. (2005). Influence of superplasticizer type and mix design parameters on the performance of them in concrete mixtures. Cement and Concrete Composites, 27(2), 217–222.

[30] Potrzebowski, J. (1983). Splitting tensile strength of steel fibre reinforced concrete. Materials and Structures, 16(2), 125–130.

[31] Qian, J., and Shi, C. (2000). High performance cementing materials from industrial slags — a review. Resources, Conservation and Recycling, 29(3), 195–207.

[32] Rubini, M., and Vijay Vikram, A. S. (2018). Effect of pozzolanas on fibre reinforced concrete. International Journal for Research in Applied Science & Engineering Technology, 6(4), 110–118.

[33] Safiuddin, M., and Hearn, N. (2005). Comparison of ASTM saturation techniques for measuring the permeable porosity of concrete. Cement and Concrete Research, 35(5), 1008–1013.

[34] Sampath Kumar, M., Venumadhav, P., and Naresh, M. (2019). Experimental study of fiber reinforced concrete using GGBS and steel fibers. International Journal for Research in Applied Science & Engineering Technology, 7(5), 201–209.

[35] Shetty, M. S. (2019). Concrete Technology: Theory and Practice. S. Chand & Company, New Delhi.

[36] Siddique, R. (2008). Waste Materials and By-Products in Concrete. Springer, Berlin.

[37] Song, P. S., Hwang, S., and Sheu, B. C. (2005). Strength properties of nylon- and polypropylene-fiber-reinforced concretes. Cement and Concrete Research, 35(8), 1546–1550.

[38] Yoo, D. Y., and Banthia, N. (2016). Mechanical properties of ultra-high-performance fiber-reinforced concrete: A review. Cement and Concrete Composites, 73, 267–280.

[39] Zain, M. F. M., Safiuddin, M., and Mahmud, H. B. (2000). Development of high performance concrete using silica fume at relatively high water-binder ratios. Cement and Concrete Research, 30(4), 635–645.

[40] Zollo, R. F. (1997). Fiber-reinforced concrete: an overview after 30 years of development. Cement and Concrete Composites, 19(2), 107–122.